



HAL
open science

Microdisplacements induced by a local perturbation inside a granular packing

Daniel Bonamy, Samuel Bernard-Bernardet, François Daviaud, Louis Laurent

► **To cite this version:**

Daniel Bonamy, Samuel Bernard-Bernardet, François Daviaud, Louis Laurent. Microdisplacements induced by a local perturbation inside a granular packing. *Physical Review E: Statistical, Nonlinear, and Soft Matter Physics*, 2003, 68 (4), pp.042301. 10.1103/PhysRevE.68.042301 . cea-01373750

HAL Id: cea-01373750

<https://cea.hal.science/cea-01373750>

Submitted on 29 Sep 2016

HAL is a multi-disciplinary open access archive for the deposit and dissemination of scientific research documents, whether they are published or not. The documents may come from teaching and research institutions in France or abroad, or from public or private research centers.

L'archive ouverte pluridisciplinaire **HAL**, est destinée au dépôt et à la diffusion de documents scientifiques de niveau recherche, publiés ou non, émanant des établissements d'enseignement et de recherche français ou étrangers, des laboratoires publics ou privés.

Microdisplacements induced by a local perturbation inside a granular packing

D. Bonamy,^{1,2} S. Bernard-Bernardet,¹ F. Daviaud,¹ and L. Laurent¹

¹*Service de Physique de l'Etat Condensé, CEA Saclay, 91191 Gif sur Yvette, France*

²*Laboratoire des Verres, Université Montpellier 2, F-34095 Montpellier Cedex 5, France*

(Received 25 October 2002; revised manuscript received 20 August 2003; published 28 October 2003)

The microdisplacements generated by a small localized overload at the free surface are visualized experimentally inside a packing of steel beads. For a triangular packing, beads rearrangements remain confined in two inverted triangles on both sides of the applied overload. This pattern disappears for stronger disorder. A simple model allows us to account for these observations and to relate them to the stress function response measured via photoelastic visualizations. This provides a different tool to probe the mechanical Green's function in weakly confined packings of rigid grains the description of which is the most challenged.

DOI: 10.1103/PhysRevE.68.042301

PACS number(s): 45.70.Qj, 45.70.Cc, 81.05.Rm

I. INTRODUCTION

Force distribution in granular packing is rather counterintuitive. For instance, the pressure profile measured at the basis of a conical sand pile can present a “dip” as well as a maximum below the apex of the heap depending on the pile construction history [1]. These results entailed intensive theoretical research, leading to several models differing significantly. A broad group of models, referred to as *elasto-plastic models*, considers granular media as elastic media as long as for any point the Mohr-Coulomb criterion is not reached [2]. In the elastic domain, the components of the stress tensor obey the *elliptic* partial differential equation (PDE). Another class of models, called oriented stress linearity (OSL) *models*, questions the existence of an elastic regime and proposes rather to put the force chain's role forward, which leads to *hyperbolic* PDE [3]. Finally, the last class of models, referred to as *q* models, assimilates the packing to a regular lattice where the force—considered only through its vertical component—is transmitted randomly from a given grain to its two neighbors beneath, which lead to *parabolic* PDE [4]. By leading to PDE of different nature, these three approaches are mutually exclusive.

How to test the competing models? The best way would be to measure the stress response function under a layer of grains of constant thickness H perturbed by the addition of an infinitesimal localized overload at the free surface; OSL models foresee that the pressure profile exhibits *two* peaks whose width increases as \sqrt{H} , separated by a distance increasing linearly with H . For the same configuration, both elastic model and *q* model predict the existence of a single peak whose width increases linearly and as square root of H , respectively. Several experiments have been performed with this aim in view using either synchro detection [5] or photoelastic visualization [6,7], but they have not allowed to clarify definitively the question. Depending on the investigated system, either the *q* model [6], the elastic model [5,7], or the OSL model [7] predictions are recovered. The stage of disorder in the packing appears as a crucial parameter [7,8], but its influence remains far from being understood.

Neither experiment [5,6] allows one to control the disorder in the packing. Moreover, the photoelastic experiments [6,7] present the drawback of considering soft grains, with a

Young modulus 10 000 times smaller than the one of steel or glass grains, while the greater sources of disagreements between the different models concern precisely the hard grains packing. In this paper, we investigate the response of steel beads packings to a localized overload at the free surface by looking at the microdisplacements rather than the stress variations within packings of different disorder stages. We show that the spatial ordering of the particle is a key parameter for the distribution of microdisplacements within the packing. Ordered packings exhibit preferential propagation direction while disordered packings do not, as what was previously observed on photoelastic visualizations [7]. The microdisplacements frames are claimed to be mainly related to the orientation map of the local forces induced by the overload. A simple model is developed to test this relationship.

II. EXPERIMENTAL SETUP

The experimental setup is illustrated in Fig. 1. It consists of a fixed drum of diameter $D_0=45$ cm and variable thickness τ , half-filled with steel beads of diameter $d=3 \pm 0.03$ mm, of Young modulus $Y=200$ GPa and of mass $m=0.11$ g. For such geometry, the stresses (resp. displacements) can be assumed to vanish at the free surface (resp. at the drum lower boundaries). Three kinds of packings are investigated: (a) a two dimensional (2D) ordered packing obtained by setting $\tau=3.05$ mm and by placing an item with a half hexagon shape in the lower half part of the drum; the

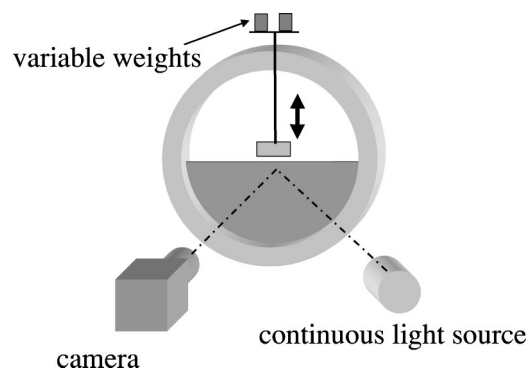


FIG. 1. Sketch of the experimental setup.

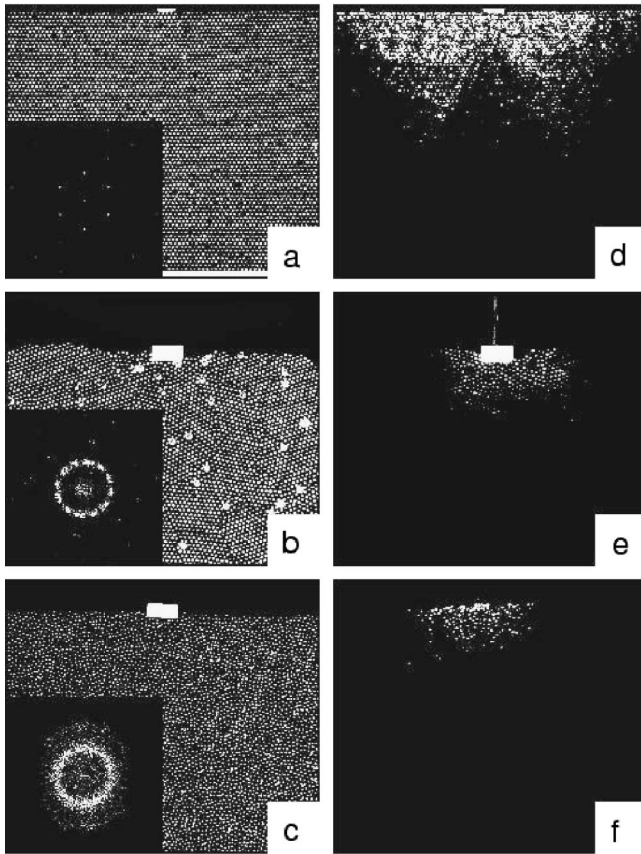


FIG. 2. Distribution of the displacements in different packing with a small overload put at the free surface. (a), (b), and (c) are the raw frames of a 1D triangular packing, a 2D disordered packing, and a quasi-2D disordered packing, respectively (see text for details). The insets present the corresponding 2D FFT transforms. The six peaks observed in (a) are the signature of the triangular packing. These peaks become blurred in the disorder 2D packing (b) and disappear in the quasi-2D packing (c). The figures (d), (e), and (f) present the displacements distribution in packings (a), (b), and (c) when an overload of mass $M=1120$ (adimensioned by the bead mass) is added at the center of the free surface.

packing is then monocrystalline with beads forming a triangular lattice [Fig. 2(a)]; (b) a 2D disordered packing by retrieving the half hexagon from the previous packing and by adding randomly 100 cylinders with diameter of 5 mm. The crystalline grains size is then about 50 beads diameters [Fig. 2(b)]; (c) a quasi-2D disordered packing by setting $\tau=7$ mm. Only beads in contact with the transparent side wall of the drum can be actually seen. This 2D cut of a 3D packing is then completely disordered [Fig. 2(c)]. The localized overload consists of a rod with a plate on which different weights can be placed at its upper tip and a pad which allows one to spread the overload on five to seven beads depending on the packing geometry at its lower tip (Fig. 1). Beads are lighted via a continuous halogen lamp. The rod is put carefully at the center of the free surface of the packing. A first sequence of 100 frames of the *constrained* packing is recorded via a fast camera at a sampling rate of 250 Hz. The rod is then retrieved very slowly. A second sequence of 100 frames of the *free* packing is recorded. The frame resolution

is 480×420 pixels, one pixel corresponding to 0.224 mm. The two sequences are first averaged. This process allows one to greatly reduce the noise caused by lighting fluctuations or drum and camera intrinsic vibrations. The two resulting frames are subtracted, and then binarized. The beads that have moved when the tube was retrieved are then distinguished. Application of this frame processing to the motion of a bead translated with a micrometric translator shows that microdisplacements superior to $20 \mu\text{m}$ are spotted unambiguously. This should be compared to the size of the cage where each bead is confined. In the packing of maximal volume fraction, the packing (a), this size is given by the scattering in the diameter and sphericity of beads, which is around $30 \mu\text{m}$. The microdisplacements entailed by the overload can then be localized but cannot be quantified. Each experiment is performed ten times by laying the rod to different places. All experimental results presented below are averaged over these ten realizations.

III. MICRODISPLACEMENTS DISTRIBUTION IN THE PACKING

Typical frames of the beads micromoved by the overload are represented in Figs. 2(d–f) for packing (a), (b), and (c), respectively. For all these packings, the number of displaced beads increases with the overload. In the ordered packing [Fig. 2(d)], moving beads stand preferentially on either side of the overload: a dark triangle, i.e., an area without any microrearrangement, can be observed at the vertical of this one. This suggests this in that kind of packing, *information* of the overload existence propagates more likely along preferential directions. Beads close to these directions feel in a stronger way the overload presence than the ones—rather closer—just below it. In the disordered packing [Figs. 2(e,f)], the triangular pattern disappears and the area sensitive to the perturbation takes the shape of a half disk. Beads are all the more liable to rearrangements as they are close to the perturbation source, without any noticeable anisotropy.

These observations can be compared to the photoelastic visualizations of Geng *et al.* [7] exhibiting a propagative component in the stress response to a point force for ordered packings whereas such stress response is more like the one of an isotropic elastic material for disordered packings. Beads microdisplacements are then conjectured to be driven by the following scenario: The overload induces an additional force component to each bead. When this last one is oriented toward the boundaries of the drum, the bead motion is only due to contact deformation (a few nanometers for grains of Young Modulus $Y=200$ GPa). Such displacements are too small to be detected by our visualization method; but when the force component is oriented toward the free surface and sufficient to lift the beads layer above it, displacements with an order of magnitude of the cage size, i.e., $30 \mu\text{m}$, are expected and can thus be detected [10].

IV. TOY MODEL

Now we propose to test this interpretation. Several models have been proposed to explain force distribution in a

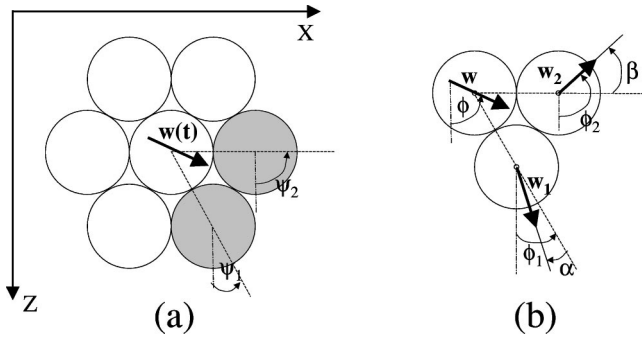


FIG. 3. Propagation rule of the overload from a given bead to two of its neighbors. (a) The orientation ϕ of the load \mathbf{w} determines the two neighbors P_1 and P_2 which will support this charge. (b) The orientations ϕ_1 and ϕ_2 of the two *children* charges resulting from the transmission coincide with the two contact orientations ψ_1 and ψ_2 at which two random numbers α and β have been added, respectively.

granular packing [4,8,9], but, to our knowledge, none of them allows one to account for beads microdisplacements. In this context, a minimal toy model has been developed. Its aim is not to reproduce quantitatively the observations, but rather to account qualitatively for the role of the disorder-controlled through a small set of parameters, ideally a single one-on both stress and displacements response functions. This model is described precisely in Ref. [11] and summarized below.

Grains are placed on a triangular lattice. Each grain is located through its coordinates (X, Z) (Fig. 3). An overload is then applied on the grain at the surface at the center of the lattice. The generated additional forces are characterized by three quantities: the position $P = (X, Z)$ of the bead to which it is applied, the norm w of the additional force and the angle Φ between this force, and the vertical (oriented from top to bottom). A force $F = 1$ is first applied to the bead O at the surface at the center of the lattice. This bead acquires an overload $\mathbf{w}(t=0)$ defined by $P = (0, 0)$, $w = F$, and $\Phi = 0$. This overload is transmitted to two of the bead neighbors at the time $t = 1$, which then transmit their overload to two of their neighbors and so on. To be more precise, at a given time t , the overload $\mathbf{w}(t) = (P, w, \Phi)$ applied to the bead $P = (X, Z)$ and created to the last time step is transmitted to the beads P_1 and P_2 associated to the contact orientation ψ_1 and ψ_2 , the closest of Φ [Fig. 3(a)]. Their locations (X_1, Z_1) and (X_2, Z_2) are thus given by $X_i = X + \sin \psi_i$, $Z_i = Z - \cos \psi_i$ for $i = \{1, 2\}$ where both X and Z are adimensioned by the bead diameter. In a triangular packing of identical perfectly smooth beads, the two transmitted overload orientation Φ_1 and Φ_2 would coincide exactly with ψ_1 and ψ_2 . To encode the disorder of the real packing as well as the existence of a friction component of the contact force and the beads polydispersity, two random angles α_1 and α_2 are added; $\Phi_i = \psi_i + \alpha_i$ for $i = \{1, 2\}$ [Fig. 3(b)]. These angles α_i are uniformly distributed between $[-\Theta, \Theta]$ where the parameter Θ quantifies the disorder stage in the simulated packing. Finally, the norms w_1 and w_2 of the transmitted loads are given by the force balance of the bead P at the time t ; $w e^{i\Phi} = w_1 e^{i\Phi_1} + w_2 e^{i\Phi_2}$.

The force network is then built in a hierarchical manner. Each overload $\mathbf{w}(t)$ has one parent and two children. The half-width L and the height H of the packing are set to $L = 100$ and $H = 100$, respectively, in bead size units. When a load reaches the boundary or the free surface, it does not propagate anymore. Boundaries are thus perfect absorbing boundaries. The number of transmitted load grows very rapidly as the network is built. A cutoff is then introduced. When the norm of a load becomes smaller than a threshold $w_c = 10^{-4}$, this does not propagate anymore. The simulation stops when all the loads are smaller than w_c .

During the simulation, a bead can get a load $w_t e^{i\Phi_t}$ at a given time t whereas it has already acquired a load $w_{t_1} e^{i\Phi_{t_1}}$ at a time t_1 anterior to t [12]. In this case, the bead will transmit only the load $w_t e^{i\Phi_t}$ since the component $w_{t_1} e^{i\Phi_{t_1}}$ has already been transmitted in the past [13]. At the end of the simulation, the final load of this bead will be the sum of all the loads $w_t e^{i\Phi_t}$ it has got during the simulation.

After the simulation completion, one gets for each bead $P = (X, Z)$ the overload given by (w, ϕ) . A new quantity δ associated to each bead is then introduced with account for the bead displacement, $\delta = 1$ when the bead has moved and $\delta = 0$ in the other case. The only free surface is for $z = 0$ where beads can move in the semi-infinite plane $z < 0$. A bead located at $P = (X, Z)$ will thus move if the z projection of its total applied force $\mathbf{w}_{total} = \mathbf{w}_0 + \mathbf{w}$ is negative (\mathbf{w}_0 corresponds to the force component applied to this bead in the absence of the surcharge). Assuming that H is large compared to the width of the zone sensitive to the overload, \mathbf{w}_0 is given on average by the hydrostatic pressure on this point: $\mathbf{w}_0 = (1/r)(2/\sqrt{3})Z$ where r denotes the ratio between the initial force $F = 1$ and the bead mass. The δ variation is then given by $\delta = 1$, when $w \sin(\phi - \pi/2) \geq (1/r)(2/\sqrt{3})Z$ and $\delta = 0$ otherwise.

A numerical experiment is thus developed according to two steps: (1) One simulates the distribution and the orientation of the overload entailed by a force $F = 1$ applied to the bead $P_0(0, 0)$. (2) The displacements entailed by these overloads are then simulated. For a given set of parameters (Θ, r) both overload and displacement field are averaged over 50 different numerical experiments.

Figures 4(a,b) present the simulated overload fields obtained for two values of Θ . For triangular packings, disorder is mainly dominated by the friction mobilization at the grain/grain contact. The angle Θ is then set to $\Theta = 5^\circ$, which corresponds to a bead/bead friction coefficient of $\mu_b = 0.1$. In the quasi-2D packing, disorder is maximal and Θ is set to $\Theta = 30^\circ$. The model captures qualitatively the behaviors observed experimentally by Geng *et al.* [7]. In a triangular packing, the perturbation propagates along two preferential contact chains which make an angle of 60° between them. In a disordered packing, these two directions exist for low depth Z , but they become blurred when Z is increased.

Figures 4(c,d) present the associated displacement field for the ordered packing ($\Theta = 5^\circ$) and the disordered packing ($\Theta = 30^\circ$), respectively. The parameter r has been set to $r = 1000$ to be compatible with our experimental measures. In the triangular packing, the triangular pattern is reproduced

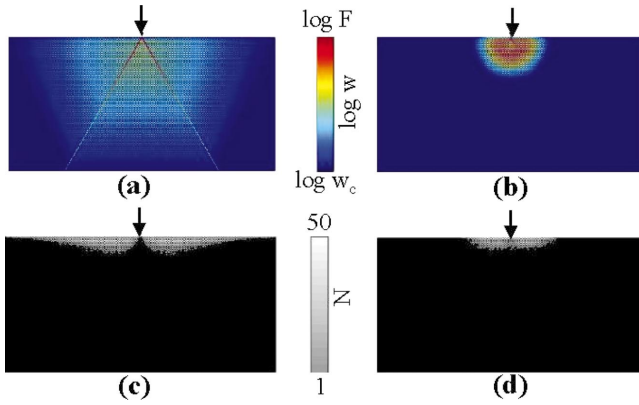


FIG. 4. (Color) Mean distribution of the overloads (top) and of the displacements (bottom) generated by the force F . Model predictions L and H have been chosen to be $L=100$ and $H=100$ and a numerical experiment is averaged over 50 realizations. Left: $\Theta = 5^\circ$. Forces propagate preferentially along two directions. Displacements are confined into two triangles on both sides of the two preferential lines. Right: $\Theta = 30^\circ$. The pattern disappears.

qualitatively with displacements localized from one part to the other of the two referential directions of force propagation. When the disorder is increased, this pattern disappears. The simulation accounts also for the fact that the extension of the area where beads can move decreases with increasing disorder. The influence of the perturbation intensity on the extension of the moving area has been also investigated, with r set to 500, 1000, and 2000 for $\Theta = 5^\circ$ [14]. These values are compatible with the ratio between the overload mass M and the beads mass investigated experimentally. In the experiment, this area extends at depth Z of $10d$, $30d$, and $35d$ for $M = 620m$, $M = 1120m$, and $M = 2180m$, respectively, while in the simulation, this area extends up to $Z = 7d$, $10d$,

and $14d$ for $r = 500$, 1000, and 2000. The correct orders of magnitude are recovered. Let us note, however that the lateral extension of the sensitive zone is much more important in the simulation than in the experiment.

V. CONCLUSION

In summary, the static of hard spheres packings has been investigated experimentally through the localization of the microdisplacements induced by a small overload added at the free surface. The spatial ordering of the grains appears as a key parameter, as previously reported by Geng *et al.* [7] concerning the stress function response in soft photoelastic grains packings. In the ordered packing, information of the surface localized overload propagates along preferential directions while the function response in disordered packings is isotropic. The microdisplacements are conjectured to be related to the orientations of the overloads induced by the perturbation, what has been tested through a toy model. Such methods allow one to probe extremely hard spheres packings contrary to photoelastic measurements and may provide a new test for the latest models [8] of static stresses distribution in granular packing. Another natural extension of this work is to investigate the microdisplacements generated by a small overload added on an *inclined* free surface. In particular, it would be very interesting to measure the change of the size of the area containing the moving beads when the inclination angle approaches the angle of repose. Work in this direction is underway.

ACKNOWLEDGMENTS

We thank O. Dauchot for fruitful discussions, and C. Gasquet, V. Padilla, and P. Meininger for technical assistance.

[1] L. Vanel *et al.*, Phys. Rev. E **60**, R5040 (1999)
 [2] K. Terzaghi, *Mcanique Thorique des Sols* (Dunod, Paris, 1951); K. Terzaghi and R.B. Peck, *Mcanique des Sols Applique* (Dunod, Paris, 1965).
 [3] J.P. Bouchaud, M.E. Cates, and P. Claudin, J. Phys. I **5**, 639 (1995); J.P. Wittmer, M.E. Cates, and P. Claudin, *ibid.* **7**, 39 (1997)
 [4] C.H. Liu *et al.*, Science **269**, 513 (1995); S.N. Coppersmith *et al.*, Phys. Rev. E **53**, 4673 (1996)
 [5] G. Reydellet and E. Clement, Phys. Rev. Lett. **86**, 3308 (2001)
 [6] M. da Silva and J. Rajchenbach, Nature (London) **406**, 708 (2000)
 [7] J.F. Geng *et al.*, Phys. Rev. Lett. **87**, 035506 (2001)
 [8] J.P. Bouchaud *et al.*, Eur. Phys. J. E **4**, 451 (2001)
 [9] P. Claudin and J.P. Bouchaud, Phys. Rev. Lett. **78**, 231 (1997); M. Nicodemi, *ibid.* **80**, 1340 (1998)
 [10] For weights of several kilograms, beads motion becomes sufficient to be measured quantitatively. Orientation of the moving beads is observed to be actually oriented toward the free surface.

[11] D. Bonamy, Ph.D. thesis, Universit Paris XI, 2001.
 [12] Such chronology implies that the sound velocity c_s is constant in the whole packing, which may appear inconsistent with the important forces variations predicted by the model. However, c_s depends weakly on stresses σ ; $c_s \propto \sigma^\alpha$ with $1/6 \leq \alpha \leq 1/4$ [X. Jia, C. Caroli, and B. Velicky, Phys. Rev. Lett. **82**, 1863 (1999)]. Consequently, it can be assumed to be constant in our minimalist model.
 [13] Let us note that, in reality, the two orientations along which the force component $w_i e^{i\Phi_i}$ is splitted are determined by the orientation of the total force $\sum_{i \leq r} w_i e^{i\Phi_i}$ applied on this grain, and not only by the orientation Φ_i . These loops were also handled by choosing the two neighbors and the two orientations among the ones determined by the previous splitting on the same bead. It does not affect the average distribution of the overload [Figs. 4(a,b)] and the displacement [Figs. 4(c,d)].
 [14] As the beads are placed on a triangular regular lattice whatever is the disorder stage in the simulation, the model predictions cannot be compared quantitatively to the experiments performed within the disordered packing.